LETTER

doi:10.1038/nature12973

Melanosome evolution indicates a key physiological shift within feathered dinosaurs

Quanguo Li[1], Julia A. Clarke[2], Ke-Qin Gao[3], Chang-Fu Zhou[4], Qingjin Meng[5], Daliang Li[6], Liliana D'Alba[7] & Matthew D. Shawkey[7]

Inference of colour patterning in extinct dinosaurs[1–3] has been based on the relationship between the morphology of melanin-containing organelles (melanosomes) and colour in extant bird feathers. When this relationship evolved relative to the origin of feathers and other novel integumentary structures, such as hair and filamentous body covering in extinct archosaurs, has not been evaluated. Here we sample melanosomes from the integument of 181 extant amniote taxa and 13 lizard, turtle, dinosaur and pterosaur fossils from the Upper-Jurassic and Lower-Cretaceous of China. We find that in the lineage leading to birds, the observed increase in the diversity of melanosome morphologies appears abruptly, near the origin of pinnate feathers in maniraptoran dinosaurs. Similarly, mammals show an increased diversity of melanosome form compared to all ectothermic amniotes. In these two clades, mammals and maniraptoran dinosaurs including birds, melanosome form and colour are linked and colour reconstruction may be possible. By contrast, melanosomes in lizard, turtle and crocodilian skin, as well as the archosaurian filamentous body coverings (dinosaur 'protofeathers' and pterosaur 'pycnofibres'), show a limited diversity of form that is uncorrelated with colour in extant taxa. These patterns may be explained by convergent changes in the key melanocortin system of mammals and birds, which is known to affect pleiotropically both melanin-based colouration and energetic processes such as metabolic rate in vertebrates[4], and may therefore support a significant physiological shift in maniraptoran dinosaurs.

Melanin-based colour is a ubiquitous feature of amniote integument, found in feathers of every major bird clade[5,6], as well as in skin and hair (the scales covering skin in reptiles are typically transparent[7]). We examined the relationship between integumentary structure and melanosome morphology in a phylogenetic context. Individual melanosomes were measured from scanning electron microscope (SEM) images of the hairs of 44 species of extant mammals ($n = 51$ samples) and the skin of 36 extant species ($n = 36$ samples), sampling across Lepidosauria, Testudines and Crocodylia (Supplementary Tables 1–3). These measurements were compared with our previously published data from 101 extant avian species ($n = 168$ feather samples[3]). Samples targeting the full range of melanin-based colours for each integument type included blacks, browns and greys for feathers, hair and skin. As feathers uniquely show a broad range of melanin-based iridescent colours, and these are known to be associated with distinctive melanosome morphologies[3], they were also included. Although iridescent colours are found in reptile skin[8] and (rarely) in hair[9], they are produced through light scattering from iridiphores and multilayer keratin films, respectively. As these colours are not melanin-based, the integuments in which they are produced were not sampled. To capture melanosome diversity fully also demanded inclusion of morphotypes associated with black colour that are so far known only from extant penguins[10].

Preserved integument from 13 fossil amniotes from the Upper Jurassic and Lower Cretaceous of northeast China were sampled using described protocols[2,3,10] (Supplementary Methods). Skin was sampled from two fossil lepidosaurs, a turtle, and two specimens of the ornithischian dinosaur *Psittacosaurus* (Extended Data Figs 1–3 and Supplementary Tables 2 and 3). Although extant amniote epidermal appendages are limited to scales, hairs and feathers[11], additional structures are observed in the fossil record. These include basally bunched or single hollow filaments in theropod dinosaurs proposed to be homologous with modern feathers[12–14], bristles and filaments in ornithischian dinosaurs[15,16], and pterosaur pycnofibres, the identity and homology of which are more controversial[17]. Filamentous structures were sampled from the theropod dinosaur *Beipiaosaurus* and two pterosaurs (Extended Data Figs 4, 5 and Supplementary Tables 2, 3). Feathers were sampled from *Caudipteryx*, *Confuciusornis*, one ornithurine and two enantiornithine birds (Extended Data Figs 2, 6–8 and Supplementary Tables 2 and 3). Published SEM images and data were assessed for filamentous structures in the non-maniraptoran coelurosaurian dinosaur *Sinosauropteryx*[1], feathers from the basal paravians *Anchiornis*[2], *Microraptor*[3] and *Archaeopteryx*[18] and

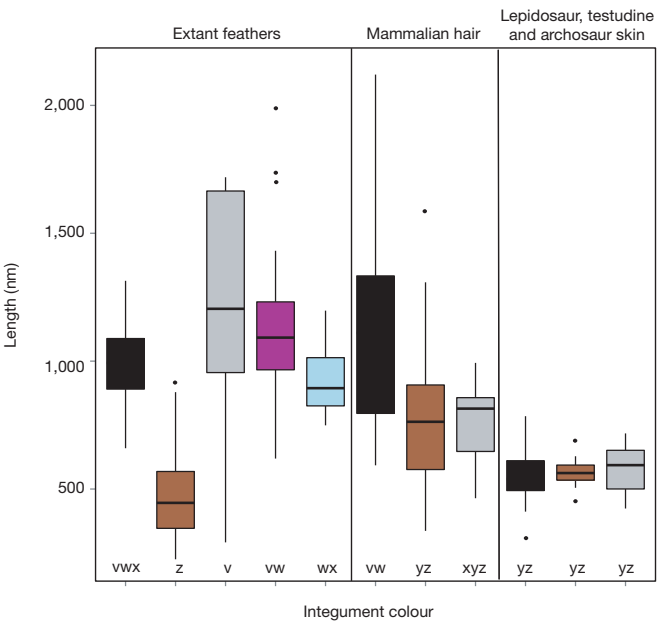

Figure 1 | Melanosome length observed in extant feathers, lepidosaur, testudine and archosaur skin, and mammalian hair. Boxplot colours correspond with integument colour: black, brown and grey. For feathers, 'penguin-like' is shown in blue, and iridescent is shown in purple. Lines are median values, boxes are quartiles, lines are range. Boxplots sharing the same letter (v, w, x, y, z) are not significantly different (two-sided Tukey HSD; $P < 0.05$) from one another; melanosome shape correlates with distinct colours in feathers and hair but not in skin. Extant feathers, $n = 168$; lepidosaur, testudine and archosaur skin, $n = 36$; mammalian hair, $n = 51$.

[1]State Key Laboratory of Biogeology and Environmental Geology, China University of Geosciences, Beijing 100083, China. [2]Department of Geological Sciences, University of Texas at Austin, 1 University Station C1100, Austin, Texas 78712, USA. [3]School of Earth and Space Sciences, Peking University, Beijing 100871, China. [4]Institute of Paleontology, Shenyang Normal University, Shenyang 110034, China. [5]Beijing Museum of Natural History, 126 Tianqiao South Street, Beijing 100050, China. [6]Museum of China University of Geosciences (Beijing), 29 Xueyuan Road, 100083, China. [7]Department of Biology and Integrated Bioscience Program, University of Akron, Akron, Ohio 44325-3908, USA.

the extinct penguin *Inkayacu*[10]. We used factorial analyses of variance (ANOVAs) and Tukey HSD (honestly significant difference) post-hoc tests in the R programming language[19] to test for differences in melanosome morphology by colour and integument type in extant samples (Fig. 1, Supplementary Methods and Extended Data Fig. 9). Canonical discriminant analysis (CDA) assessed the accuracy of the colours predicted for extant skin and hair samples based on melansome morphology (Supplementary Methods).

Across extant Amniota, the range of melanosome shape and form differs between taxa and integumentary types (Figs 1–4). These differences are directly related to the ability to predict colour from melanosome morphology (Supplementary Methods). For example, unlike in extant bird feathers[1–3], extant lepidosaur, turtle and crocodilian skin colour cannot be predicted from morphology alone (Fig. 1; Supplementary Methods). Diversity of melanosome morphology in these taxa is limited (Figs 1 and 2a, b) compared to mammals and birds (Figs 2c–f and 4). Although CDA analyses of extant feathers classify colours with 82% accuracy based on morphology[3], no two colours of skin could be discriminated. Indeed, because no morphological variable was correlated with colour in extant skin, none could be used in CDA (Supplementary methods). Overall, melanosome length was more variable than diameter within and among amniote integument types. For hair (Fig. 2c, d), a CDA with melanosome length as a variable weakly predicted colour when grey hairs were included (59% accuracy), but predicted colour well (87% accuracy) when they were excluded (Supplementary Methods). This is likely because, in contrast to grey feathers, grey hair is typically produced by macroscale patterns of alternating dark and light hairs or striping within single hairs, rather than associated with distinct melanosome shapes[7] (Supplementary Methods).

Only two shifts in integumentary structure in amniotes, the origin of pinnate feathers and mammalian hairs, are associated with shifts in melanosome diversity (Fig. 4). CDA indicates that colour and melanosome morphology are linked in the extant parts of these clades (Supplementary Methods). By contrast, no similar shift is observed in the transition to filamentous integument in archosaurs or in the transition from single hollow filaments to branched and basally joined bundles of filaments in Coelurosauria[15] (Fig. 4). If the structures in pterosaurs, ornithischian dinosaurs and theropods represent three separate origins of filamentous structures instead of one early in Archosauria, this pattern

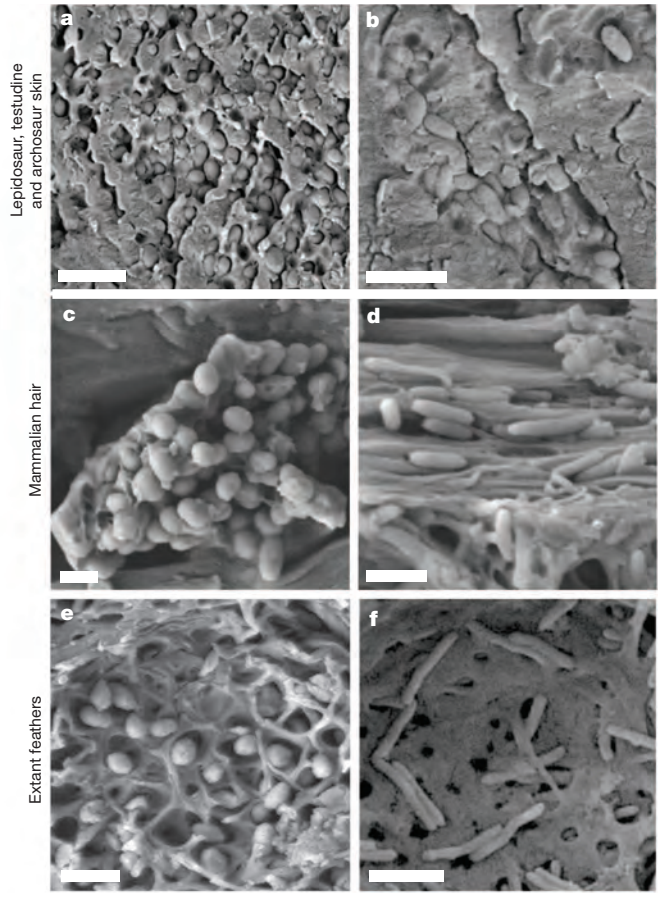

Figure 2 | SEM images of melanosomes from extant taxa representing the lowest-aspect-ratio and highest-aspect-ratio forms for each integumentary type. **a**, **b**, Skin of leaf-tailed gecko, *Uroplatus fantasticus* (**a**), and Galapagos fire lizard, *Microlophus albemarlensis* (**b**). **c**, **d**, Hair from hairy-tailed mole, *Parascalops breweri* (**c**), and domestic cat, *Felis catus* (**d**). **e**, **f**, Feathers from tufted titmouse, *Baeolophus bicolor* (**e**), and Huon astrapia, *Astrapia rothschildi* (**f**). Scale bars, 1 μm.

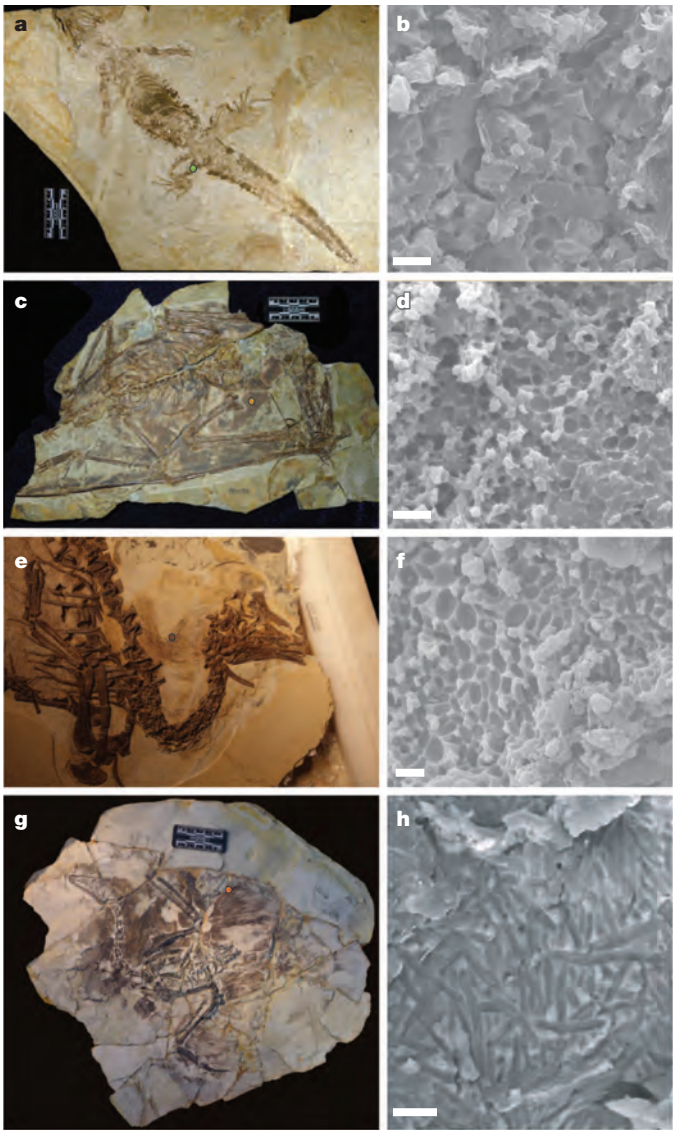

Figure 3 | Melanosomes from Jehol Group fossils. **a**–**h**, Images show the differences between low-aspect melanosomes consistently observed in lepidosaur skin (PKUP V1059; **a**, **b**) and filamentous structures in pterosaurs (BMNHC PH000988; **c**, **d**); and between non-maniraptoran dinosaurs (*Beipiaosaurus*; BMNHC PH000911; **e**, **f**) and the high-aspect-ratio forms observed in maniraptoran feathers (undescribed ornithurine bird, CUGB G20100053; **g**, **h**). Dots in **a**, **c**, **e** and **g** indicate the location of the samples shown in **b**, **d**, **f** and **h**. Dot colours correspond to the colours in Fig. 4: light green, extinct lepidosaurian, testudine and crocodilian skin; dark brown, filamenous body covering in dinosaurs; light brown, pterosaurs; orange, feathers in extinct stem avialan taxa. See Extended Data Figures for complete sampling maps. Scale bars, 1 μm.

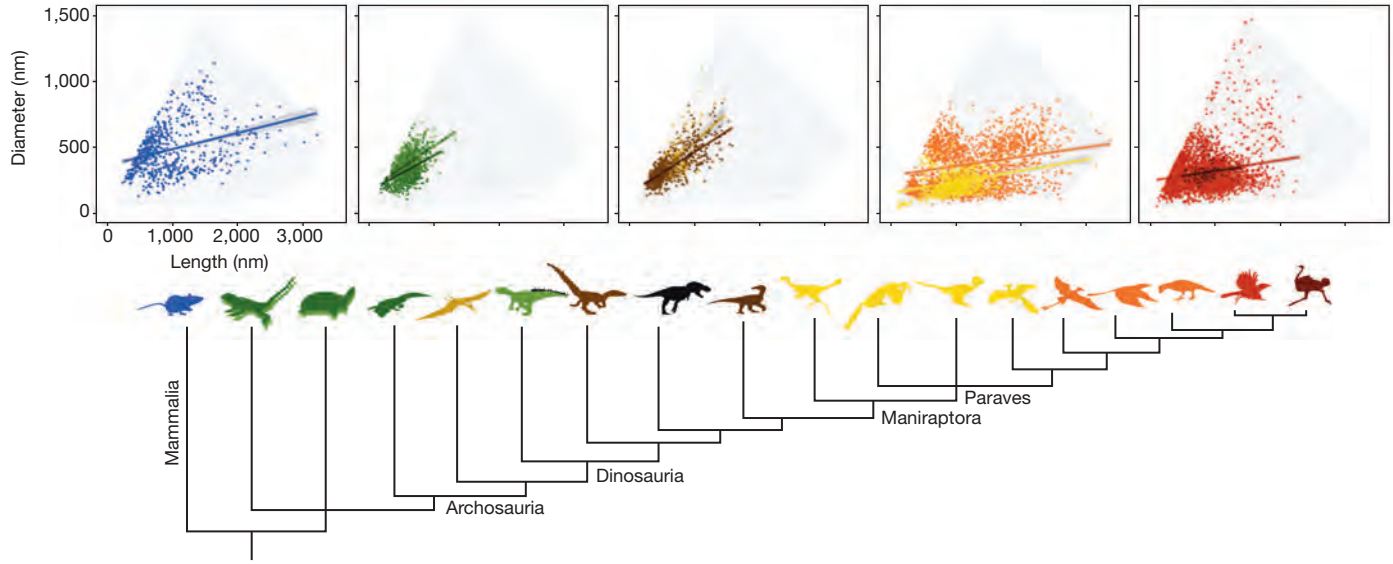

Figure 4 | Melanosome diversity across Amniota. Scatterplots of individual melanosome measurements (diameters and lengths) by integument type for extant mammal hair (blue, $n = 719$), skin from extant (dark green, $n = 742$) and extinct (light green, $n = 925$) lepidosaurian, testudine and archosaurian species, filamentous body covering in pterosaurs (light brown, $n = 899$), filamentous body covering in dinosaurs (dark brown, $n = 164$), feathers in basal Paraves (yellow, $n = 1,268$), *Confuciusornis* and crown-ward extinct avialan taxa (orange, $n = 1,683$), extant Aves (bright red, $n = 3,294$) and flightless palaeognath birds (dark red, $n = 107$). Colours of silhouettes correspond with colours in scatterplots. Black indicated unsampled taxa or integumentary type (e.g., bristle structures on the tail of *Psittacosaurus*). Grey regions in scatterplots indicate the extent of melanosome diversity in all samples (total observed melanosome morphospace), and regression lines are drawn for comparison among integumentary types. Shaded areas around lines indicate 95% confidence intervals.

would be even stronger. Observed melanosome size and variation were similar in extinct and extant taxa of each major amniote group and for each integumentary type (for example, extant and fossil skin) (Figs 2–4). Accounting for proposed taphonomic alteration of fossil melanosome size (that is, average 18–20% reduction in size[20]) does not affect recovered patterns (Extended Data Fig. 10; compare with Fig. 4). Indeed, fit of sampled fossil lepidosaur, testudine and archosaur melanosomes with extant taxa argues against significant taphonomic alteration (see also Supplementary Methods).

Pterosaurs and non-maniraptoran dinosaurs show a limited range of low-aspect-ratio (length:width, <2) melanosome morphologies (Figs 3c–f and 4) similar to the morphospace occupied by fossil and extant lepidosaurs, crocodylians and turtles (Figs 3a, b and 4). Low-aspect-ratio melanosomes in *Sinosauropteryx* filaments have been interpreted as indicative of a reddish brown colour based on avian comparisons[1]. By this logic the newly sampled pterosaurs and *Beipiaosaurus* (Fig. 3c, f and Extended Data Figs 4 and 5) would all be inferred as similarly brown (avian CDA; Supplementary Methods). However, plesiomorphically, low-aspect-ratio melanosomes from skin (Fig. 2a, b) produce black, brown or grey colours, and there is no evidence that derived avian relationships between shape and colour apply to more basal taxa occupying a similar (outgroup) melanosome morphospace (Fig. 1, Extended Data Fig. 9 and Supplementary Table 2). Colour reconstruction for these archosaurian taxa based on melanosome morphology is therefore cautioned against.

Melanosome diversity in Amniota does not track novelties in the material of which these integumentary structures are comprised, previously proposed differences in melanin chemistry, or the range of colours produced (Fig. 4). In terms of novelties in material, novel β-keratins arose in both Lepidosauria and Testudines, some are shared by birds and crocodilians, and some are unique to birds[21]. However, only those unique to birds may be associated with observed changes in the melanin system. Mammalian hair consists of structurally distinct α-keratin but exhibits melanosome diversity approaching that in birds (Figs 2 and 4). In terms of previously proposed differences in melanin chemistry, although phaeomelanin was long thought to be exclusive to mammals and birds[22], it has recently been reported in amphibians[23] and turtles[24], and thus its distribution does not explain the recovered differences in melanosome diversity. Finally, in terms of the range of colours produced, colouration is a key function of melanin in amniotes and the range of colours across our sampled taxa vary markedly. However, melanosome diversity in amniotes is not predicted by how colourful the extant parts of these taxa are today. Lepidosaurs show low melanosome diversity and brightly coloured species make use of other colour-producing mechanisms[8]. Mammals generally exhibit more muted colours than those observed in birds and lack structural colouration other than a weak iridescence produced by a keratin multilayer in golden moles[9]. However, they show a striking diversity of melanosome morphologies, most similar to the range observed in birds (Fig. 4).

Shifts in the melanin-based colour system in amniotes may instead be explained by physiological innovations. Convergent changes in the melanin-based colour system towards an expanded range of melanosome lengths, diameters and aspect ratios occur in maniraptoran dinosaurs and in mammals (Figs 2–4). Interactions between the agouti signalling protein (ASIP) and the melanocortin 1 receptor (MC1R) have been implicated in shifts in melanin synthesis in developing feathers[25] as well as hair[26]. Within-feather patterning, such as stripes, results from these interactions[25,26] and first appears within maniraptoran dinosaurs[1] coincident with the increase in melanosome diversity noted here (Fig. 4). The changes we observe are thus consistent with independent shifts in at least these axes of the melanocortin system in the lineages leading to mammals and birds.

The melanocortin system pleiotropically affects both melanin-based colouration as well as key energetic processes such as metabolic rate, reproductive physiology, stress axis and food intake across vertebrates (from bony fish to humans[4,27,28]). In Aves, inter- and intraspecific variation in melanic colour has been linked to differences in energetics and metabolism[4,27], and a possible role of convertase enzymes PC1/3 and PC2 was recently implicated in pleiotropic effects[28]. ASIP also has well-characterized pleiotropic effects[27], and in particular the ASIP–MC1R interaction was recently recognized to have a physiological as well as pigmentary role in birds[29]. Mirroring the broad patterns between ecto- and endothermic animals, our results show that avian taxa that exhibit

lower basal metabolic rates, flightless paleognaths[30], also exhibit lower melanosome diversity (Fig. 4). The fact that melanosome diversity in endothermic extant amniotes is similar, despite profound differences in keratin chemistry[21], integumentary structure and melanocortin pathways[4,27], may be because melanosome diversity is pleiotropically linked to changes in energetics associated with the higher metabolic rates they uniquely share. Although further investigation is clearly required, the change in melanin-based colour reported here, and the origin of within-feather melanin-based colouration in Maniraptora[1], may indicate when a key shift in dinosaurian physiology occurred before the origin of flight.

METHODS SUMMARY

We obtained data on melanosome morphology from extant hair and skin samples using techniques previously described for feathers[3]. In brief, hair and skin samples were embedded in plastic and sectioned longitudinally with a glass knife on an ultramicrotome. These sections were viewed on a JEOL JSM7401F SEM. The image-processing program ImageJ (available for download at http://rsbweb.nih.gov/ij/) was used to measure length, diameter, aspect ratio and density in SEM images acquired. We used ANOVA and Tukey post-hoc tests to compare these variables between integumentary type, and a canonical discriminant analysis to determine whether colour of skin or hair could be predicted from these morphological variables. We took small (approximately 1 mm^2) samples from a range of integumentary structures in the fossil record, including feathers, skin, 'pycnofibres' and 'proto-feathers' and viewed them on a ZEISS SUPRA-55 VP SEM. Melanosome morphology data were collected from these samples using ImageJ. We visualized all data using the *ggplot2* package in R[19].

Online Content Any additional Methods, Extended Data display items and Source Data are available in the online version of the paper; references unique to these sections appear only in the online paper.

Received 21 October; accepted 20 December 2013.

Published online 12 February 2014.

1. Zhang, F. *et al.* Fossilized melanosomes and the colour of Cretaceous dinosaurs and birds. *Nature* **463,** 1075–1078 (2010).
2. Li, Q. *et al.* Plumage color patterns of an extinct dinosaur. *Science* **327,** 1369–1372 (2010).
3. Li, Q. *et al.* Reconstruction of *Microraptor* and the evolution of iridescent plumage. *Science* **335,** 1215–1219 (2012).
4. Ducrest, A.-L., Keller, L. & Roulin, A. Pleiotropy in the melanocortin system, coloration and behavioural syndromes. *Trends Ecol. Evol.* **23,** 502–510 (2008).
5. Stoddard, M. C. & Prum, R. O. How colorful are birds? Evolution of the avian plumage color gamut. *Behav. Ecol.* **22,** 1042–1052 (2011).
6. McGraw, K. J. in *Bird Coloration. 1. Mechanisms and Measurements* (eds Hill, G. E. & McGraw, K. J.) 243–294 (Harvard Univ. Press, 2006).
7. Mills, M. G. & Patterson, L. B. Not just black and white: pigment pattern development and evolution in vertebrates. *Semin. Cell Dev. Biol.* **20,** 72–81 (2009).
8. Bagnara, J. T. & Hadley, M. E. *Chromatophores and Color Change: The Comparative Physiology of Animal Pigmentation* (Prentice-Hall, 1973).
9. Snyder, H. K. *et al.* Iridescent colour production in hairs of blind golden moles (Chrysochloridae). *Biol. Lett.* **8,** 393–396 (2012).
10. Clarke, J. A. *et al.* Fossil evidence for evolution of the shape and color of penguin feathers. *Science* **330,** 954–957 (2010).
11. Spearman, R. I. C. *The Integument* (Cambridge Univ. Press, 1973).
12. Xu, X., Zhou, Z. & Prum, R. O. Branched integumental structures in *Sinornithosaurus* and the origin of feathers. *Nature* **410,** 200–204 (2001).
13. Xu, X. *et al.* Basal tyrannosauroids from China and evidence for protofeathers in tyrannosauroids. *Nature* **431,** 680–684 (2004).
14. Ji, Q., Norell, M. A., Gao, K.-Q., Ji, S.-A. & Ren, D. The distribution of integumentary structures in a feathered dinosaur. *Nature* **410,** 1084–1088 (2001).
15. Zheng, X.-T., You, H.-L., Xu, X. & Dong, Z.-M. An Early Cretaceous heterodontosaurid dinosaur with filamentous integumentary structures. *Nature* **458,** 333–336 (2009).
16. Mayr, G., Peters, D. S., Plodowski, G. & Vogel, O. Bristle-like integumentary structures at the tail of the horned dinosaur *Psittacosaurus*. *Naturwissenschaften* **89,** 361–365 (2002).
17. Kellner, A. W. A. *et al.* The soft tissue of *Jeholopterus* (Pterosauria, Anurognathidae, Batrachognathinae) and the structure of the pterosaur wing membrane. *Proc. R. Soc. Lond. B* **277,** 321–329 (2010).
18. Carney, R., Vinther, J., Shawkey, M. D., D'Alba, L. & Ackermann, J. New evidence on the colour and nature of the isolated *Archaeopteryx* feather. *Nature Comm.* **3,** 637 (2012).
19. R Development Core Team. R: A language and environment for statistical computing. (R Foundation for Statistical Computing, 2008).
20. McNamara, M. E., Briggs, D. E. G., Orr, P. J., Field, D. J. & Wang, Z. Experimental maturation of feathers: implications for reconstructions of fossil feather colour. *Biol. Lett.* **9,** 20130184.
21. Greenwold, M. H. & Sawyer, R. H. Linking the molecular evolution of avian beta (β) keratins to the evolution of feathers. *J. Exp. Zool. Mol. Dev. Evol.* **316,** 609–616 (2011).
22. Ito, S. & Wakamatsu, K. Quantitative analysis of eumelanin and pheomelanin in humans, mice, and other animals. *Pigment Cell Res.* **16,** 523–531 (2003).
23. Wolnicka-Glubisz, A., Peclo, A., Podkowa, D., Kolodziejczyk, L. M. & Plonka, P. M. Pheomelanin in the skin of *Hymenochirus boettgeri* (Amphibia:Anura:Pipidae). *Exp. Dermatol.* **21,** 537–540 (2012).
24. Roulin, A., Mafli, A. & Wakamatsu, K. Reptiles produce pheomelanin: evidence in the Eastern Hermann's Tortoise. *J. Herpetol.* **47,** 258–261 (2013).
25. Yoshihara, C. *et al.* Elaborate color patterns of individual chicken feathers may be formed by the agouti signaling protein. *Gen. Comp. Endocrinol.* **175,** 495–499 (2012).
26. Manceau, M., Domingues, V. S., Mallarino, R. & Hoekstra, H. E. The developmental role of agouti in color pattern evolution. *Science* **331,** 1062–1065 (2011).
27. Hubbard, J. K., Uy, J. A. C., Hauber, M. E., Hoekstra, H. E. & Safran, R. J. Vertebrate pigmentation: from underlying genes to adaptive function. *Trends Genet.* **26,** 231–239 (2010).
28. Emaresi, G. *et al.* Pleiotropy in the melanocortin system: expression levels of this system are associated with melanogenesis and pigmentation in the tawny owl (*Strix aluco*). *Mol. Ecol.* **22,** 4915–4930 (2013).
29. Yabuuchi, M., Bando, K., Hiramatsu, M., Takahashi, S. & Takeuchi, S. Local agouti signaling protein/melanocortin signaling system that possibly regulates lipid metabolism in adipose tissues of chickens. *J. Poult. Sci.* **47,** 176–182 (2010).
30. Calder, W. A., III & Dawson, T. J. Resting metabolic rates of ratite birds: the kiwis and the emu. *Biochem. Physiol. A* **60,** 479–481 (1978).

Supplementary Information is available in the online version of the paper.

Acknowledgements This work was supported by the National Natural Science Foundation of China (NSFC) grant 41272031, Fundamental Research Funds for Central Universities, Beijing Municipal Bureau of Human Resources, NSF grants EAR-1251895 and 1251922, Human Frontier Science Program (HFSP) grant RGY-0083, Air Force Office of Scientific Research (AFOSR) grant FA9550-13-1-0222, and the Jurassic Foundation. The Smithsonian Institution (J. F. Jacobs and A. Wynn) and San Diego Museum of Natural History (P. Unitt) provided extant samples. BMNHC PH000911 was photographed by M. Ellison.

Author Contributions J.A.C., K.-Q.G., Q.L. and M.D.S. (listed alphabetically) jointly conceived the study and participated in manuscript preparation. Data for extant taxa were collected by L.D. and M.D.S. Data from fossil taxa were collected by Q.L., M.D.S., J.A.C., K.-Q.G., C.-F.Z., L.D. and Q.M. Data collection from fossils was supervised by Q.L., Q.M, C.-F.Z. and D.L.; J.A.C. and M.D.S. developed the analytical approach and assessed results jointly with Q.L. and K.-Q.G.; M.D.S, L.D. and Q.L. analysed the data.

Author Information Specimens are permanently reposited at the public institutions indicated in the text and Supplementary Table 3; sampling is illustrated in the Extended Data Figures, and melanosome data are given in Supplementary Table 2 or have been made available previously[3]. Reprints and permissions information is available at www.nature.com/reprints. The authors declare no competing financial interests. Readers are welcome to comment on the online version of the paper. Correspondence and requests for materials should be addressed to J.A.C. (Julia_Clarke@jsg.utexas.edu) or M.D.S. (shawkey@uakron.edu).

METHODS

Samples of extant amniote integument were used to capture the diversity of melanosomes associated with melanin-based colours found in each clade (see Supplementary Methods for details). Extant hairs were pulled from study specimens of mammals in the collections of the University of Akron and the San Diego Museum of Natural History, and small (approximately 5 mm^2) sections of skin were cut from melanized portions near the forelimb of formalin-preserved reptiles in the collection of the Smithsonian Museum of Natural History. Sampled species are listed in Supplementary Table 2. We obtained data on melanosome morphology from these samples as described previously[3]. First, skin or hair was embedded in Epon by dehydration using 100% ethanol (20 min) twice, and by infiltration with 15, 50, 70 and 100% Epon (24 h each step). Infiltrated samples were then placed in block moulds and polymerized at 60 °C for 16 h. We then cut thick (5 μm) longitudinal sections of blocks with a glass knife on a Leica UC-6 ultramicrotome, mounted them on stubs with carbon tape, sputter-coated them with silver and viewed them on a JEOL JSM7401F SEM.

From the resulting SEM images we used the image-processing program ImageJ (available for download at http://rsbweb.nih.gov/ij/) to measure melanosome morphology as described previously[3]. We measured maximum linear short and long axis length of melanosomes that were oriented perpendicular to line of sight, and from these data calculated aspect ratio (long:short axis). These ratios are an index of shape, and values close to 1 indicate sphericity, whereas values further from 1 indicate cylindricity. The distribution of melanosome morphology within feathers was frequently skewed towards one type of morphology, therefore we also calculated the skewness of the long and short axes. We calculated density as the number of melanosomes per square micron of integumentary surface area. Using the R environment, we compared these values between extant coloured integument using ANOVA (aov function) and Tukey's post-hoc test (Tukey HSD function). Results are summarized in Fig. 1 and Supplementary Table 1.

We used a quadratic canonical discriminant analysis to determine whether colour could be predicted from melanosome morphology in hair and skin. We used a quadratic rather than linear discriminant analysis because some variables showed evidence of collinearity, but use of linear discriminant analysis did not significantly alter results. We used a forward stepwise method to choose variables that contributed significantly ($P < 0.05$) to the analysis and to eliminate those that did not.

We sampled fossils with preserved integument spanning the range of known forms, including skin, 'protofeathers', 'pycnofibres' and pinnate feathers. We collected morphological data from SEM images of fossil integument from the Jehol biota in the same manner as the extant samples. Small (approximately 1 mm^2) samples were taken from preserved integument of fossils as before[3]. Each specimen was sampled as thoroughly as possible to maximize the potential diversity of melanosomes while maintaining the integrity of the fossil. The samples were coated with silver (30 s) and studied with either a ZEISS SUPRA-55 VP field emission scanning electron microscope (situated at China University of Geosciences, Beijing) or the JEOL environmental scanning electron microscope used for extant samples. Morphological measurements from melanosomes preserved as imprints and in three dimensions were assembled in the same manner as the modern samples. There was no taxonomic variation in the frequency of distinct preservational styles. These data are summarized in Fig. 3 and Supplementary Table 3.

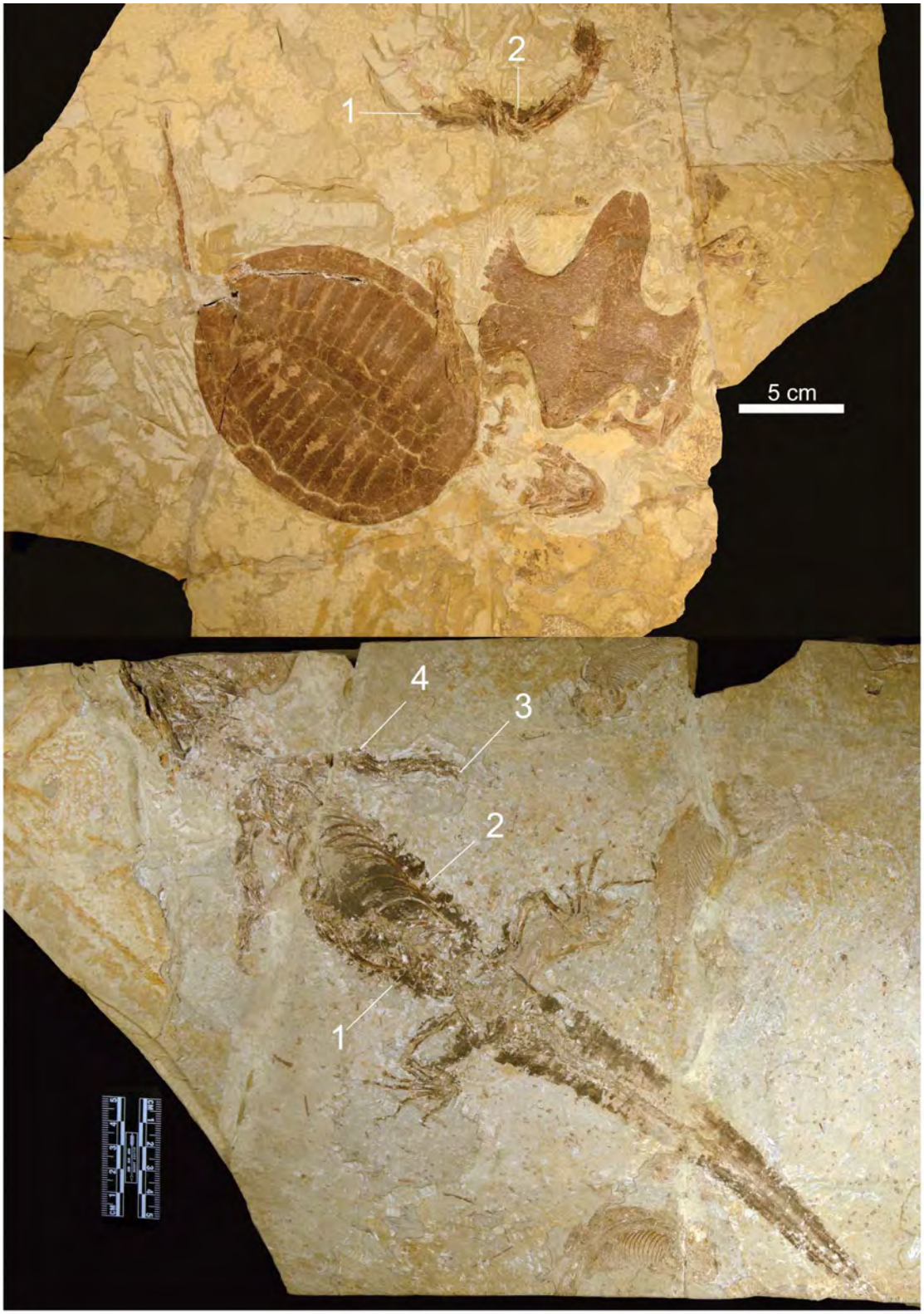

Extended Data Figure 1 | Sampling map of an unnamed turtle fossil, PKUP V1070 (top) and a lizard fossil, *Yabeinosaurus sp.* PKUP V1059 (bottom). Numbers indicate integument sampling sites; melanosome data from all sites are presented in Fig. 4 and pooled for the per-taxon values given in Supplementary Table 2.

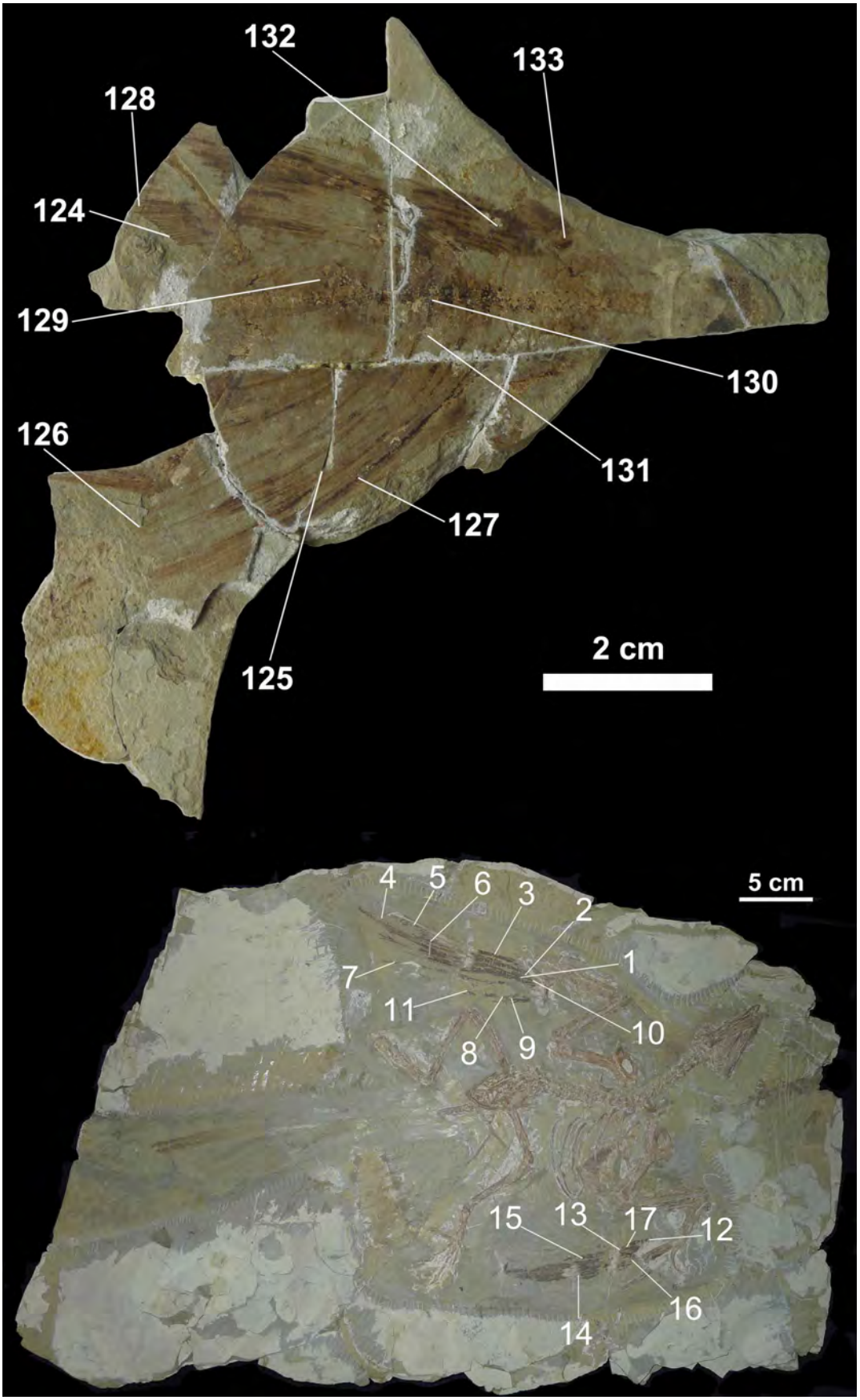

Extended Data Figure 2 | Sampling map of a gliding lizard fossil, *Xianglong zhaoi*, PMOL 000666, counterpart (top) and the basal avialan, *Confuciusornis sanctus*, CUGB G20070001 (bottom). Integument sampling sites are numbered. Numbers indicate integument sampling sites; melanosome data from all sites are presented in Fig. 4 and pooled for the per-taxon values given in Supplementary Table 2.

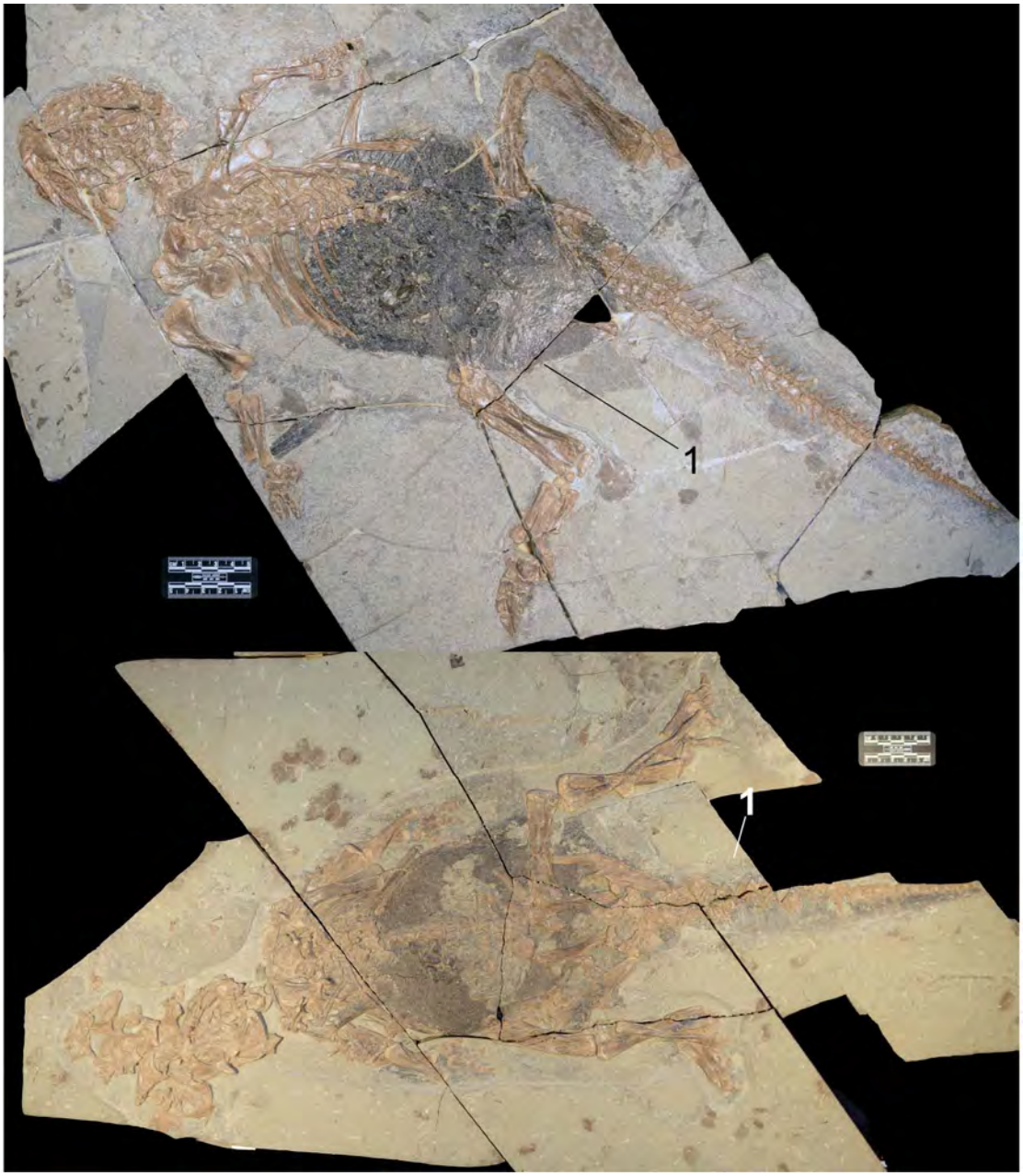

Extended Data Figure 3 | Skin sample from the ornithischian dinosaur, *Psittacosaurus lujiatunensis*, PKUP V1050 (top) and from the ornithischian dinosaur, *Psittacosaurus lujiatunensis*, PKUP V1051 (bottom). Numbers indicate integument sampling sites; melanosome data from all sites are presented in Fig. 4 and pooled for the per-taxon values given in Supplementary Table 2.

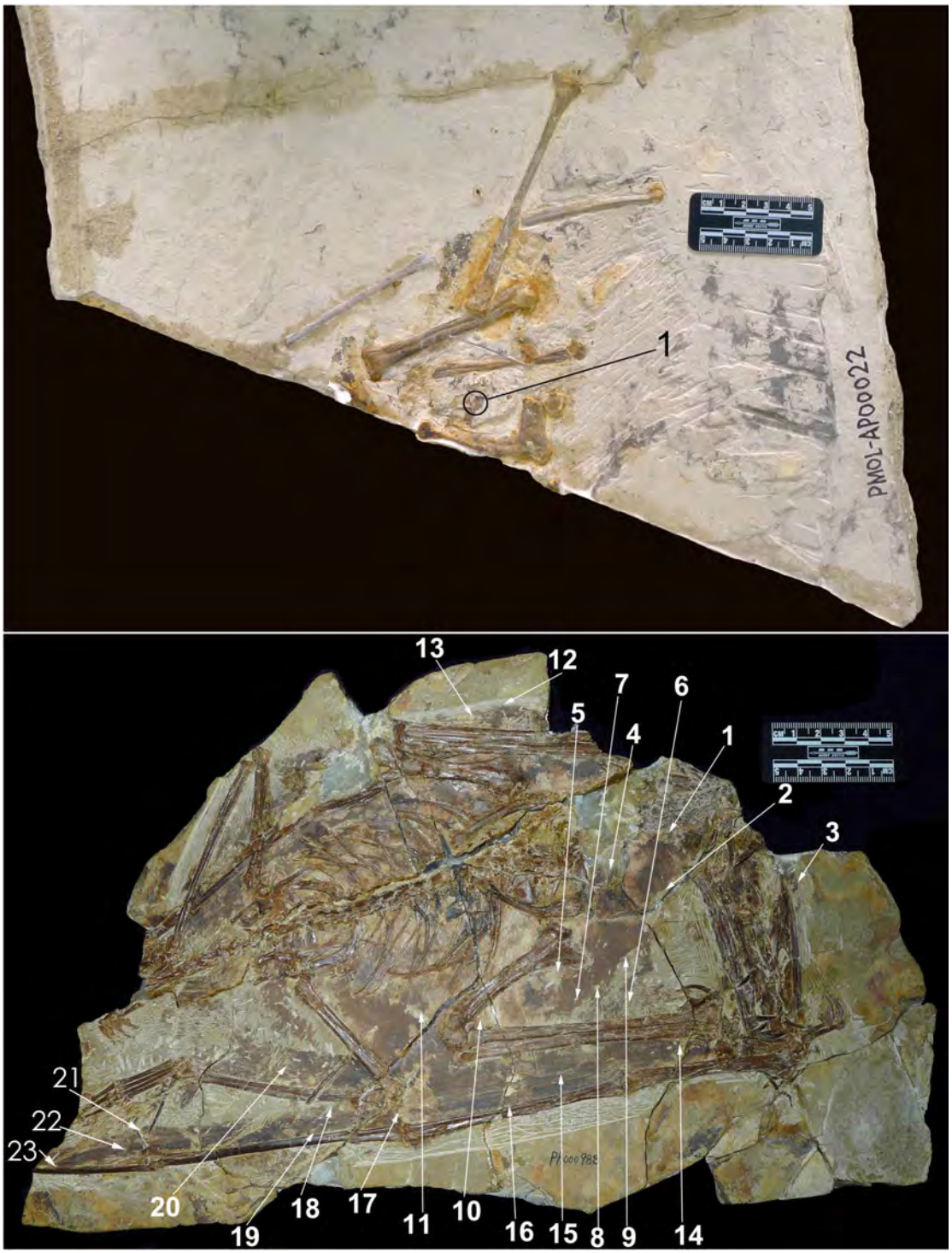

Extended Data Figure 4 | Sampling map for two pterosaurs, PMOL AP00022 (top) and BMNHC PH000988 (bottom). Numbers indicate integument sampling sites; melanosome data from all sites are presented in Fig. 4 and pooled for the per-taxon values given in Supplementary Table 2.

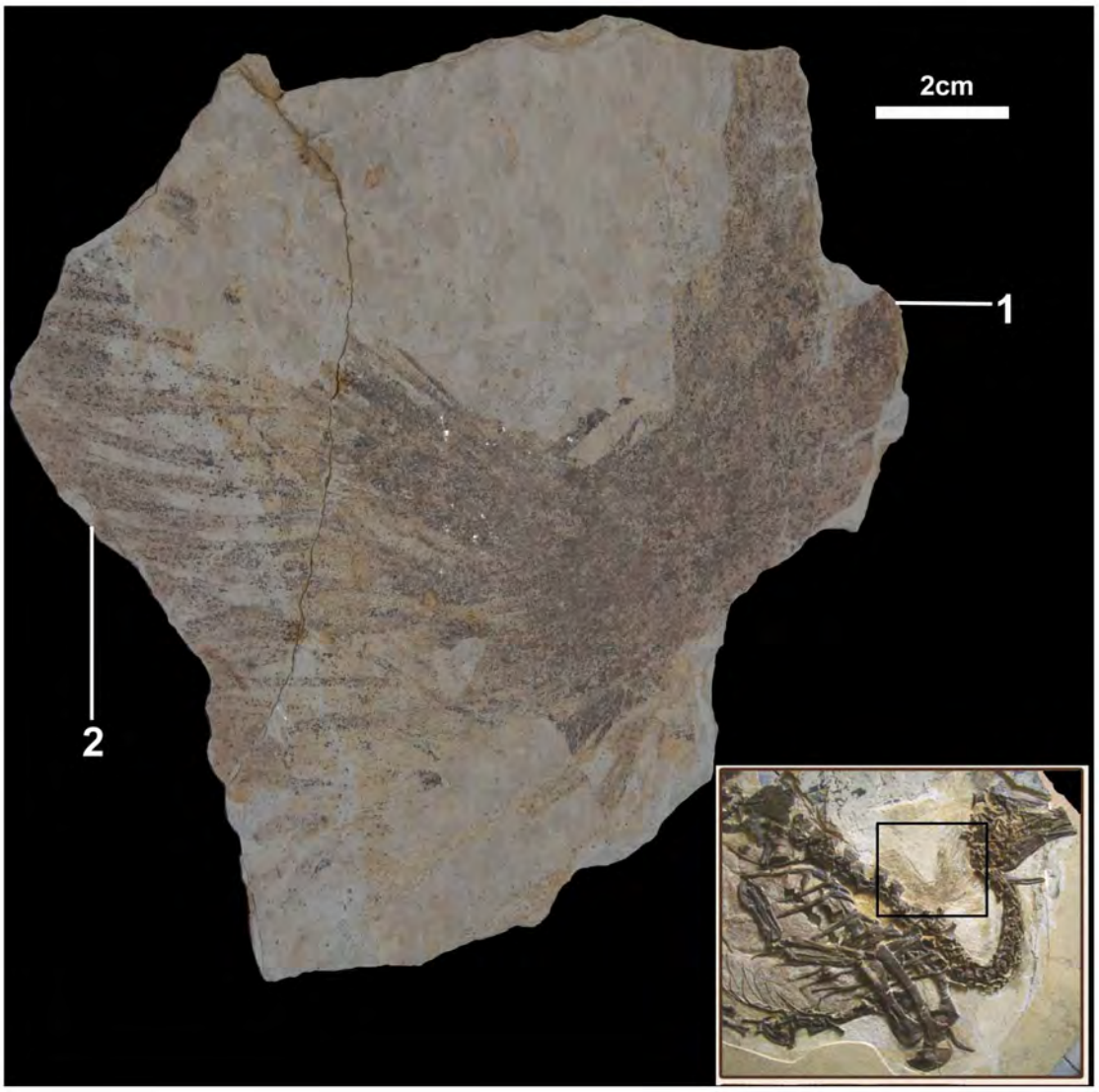

Extended Data Figure 5 | Samples from filaments preserved in the neck region of a skeleton of the theropod dinosaur, *Beipiaosaurus*, BMNHC PH000911 (counter slab). Numbers indicate integument sampling sites; melanosome data from all sites are presented in Fig. 4 and pooled for the per-taxon values given in Supplementary Table 2.

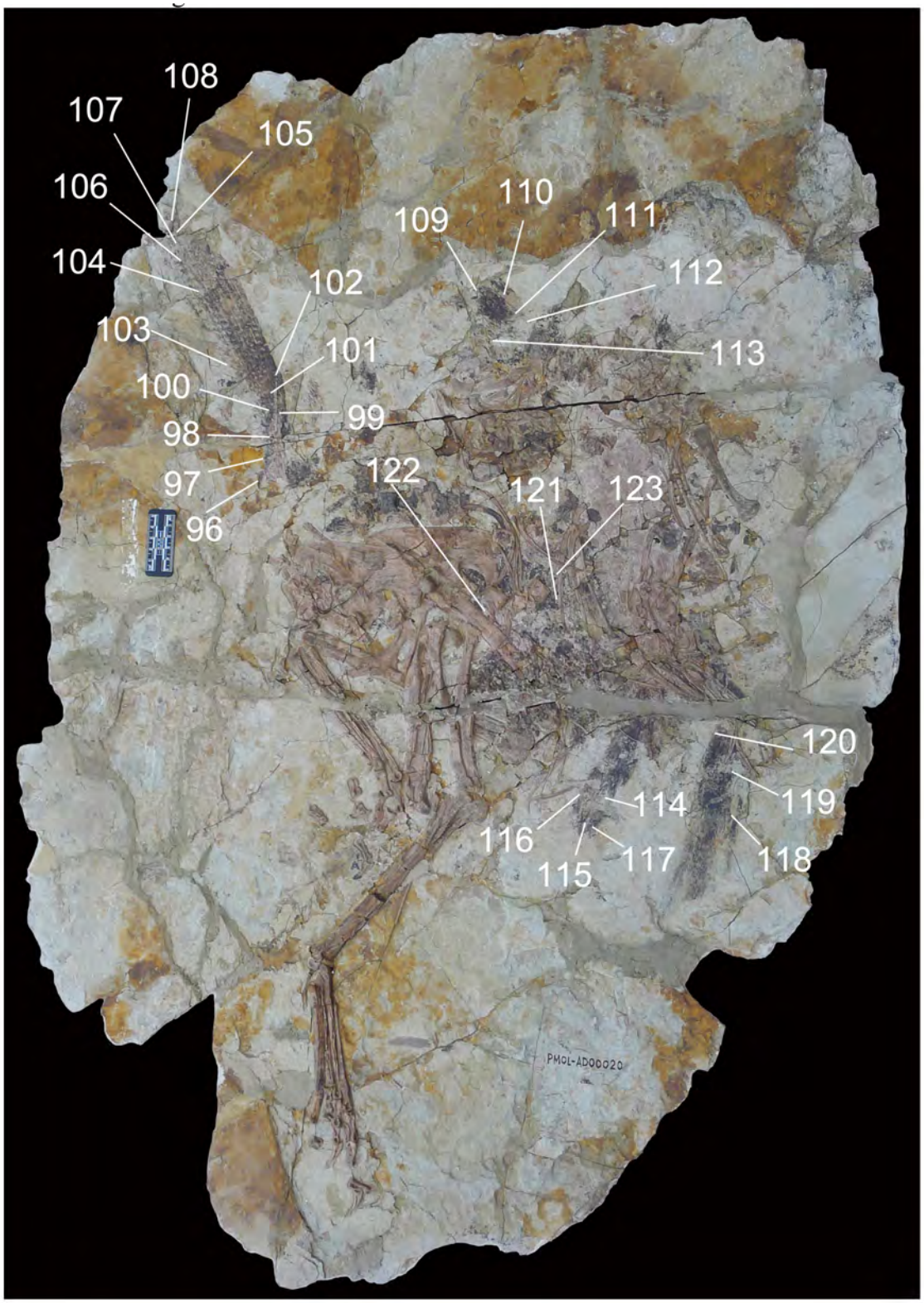

Extended Data Figure 6 | Sampling map of the feathered maniraptoran dinosaur, *Caudipteryx zoui*, PMOL AD00020. Numbers indicate integument sampling sites; melanosome data from all sites are presented in Fig. 4 and pooled for the per-taxon values given in Supplementary Table 2.

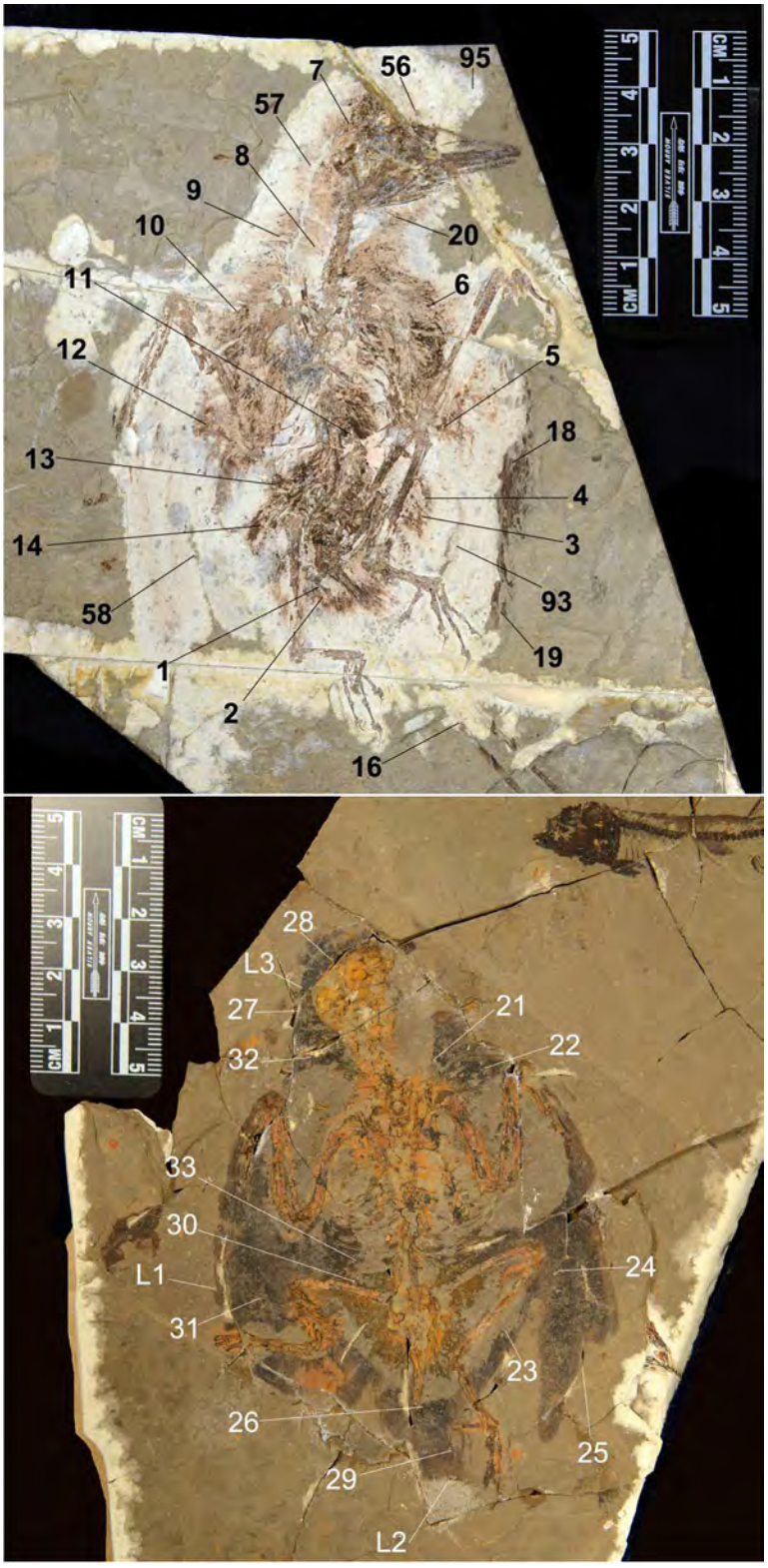

Extended Data Figure 7 | Sampling map of (top) an unnamed enantiornithine bird, CUGB G20120001 and (bottom) an undescribed enantiornithine bird, CUGB P1201. Numbers indicate integument sampling sites; melanosome data from all sites are presented in Fig. 4 and pooled for the per-taxon values given in Supplementary Table 2.

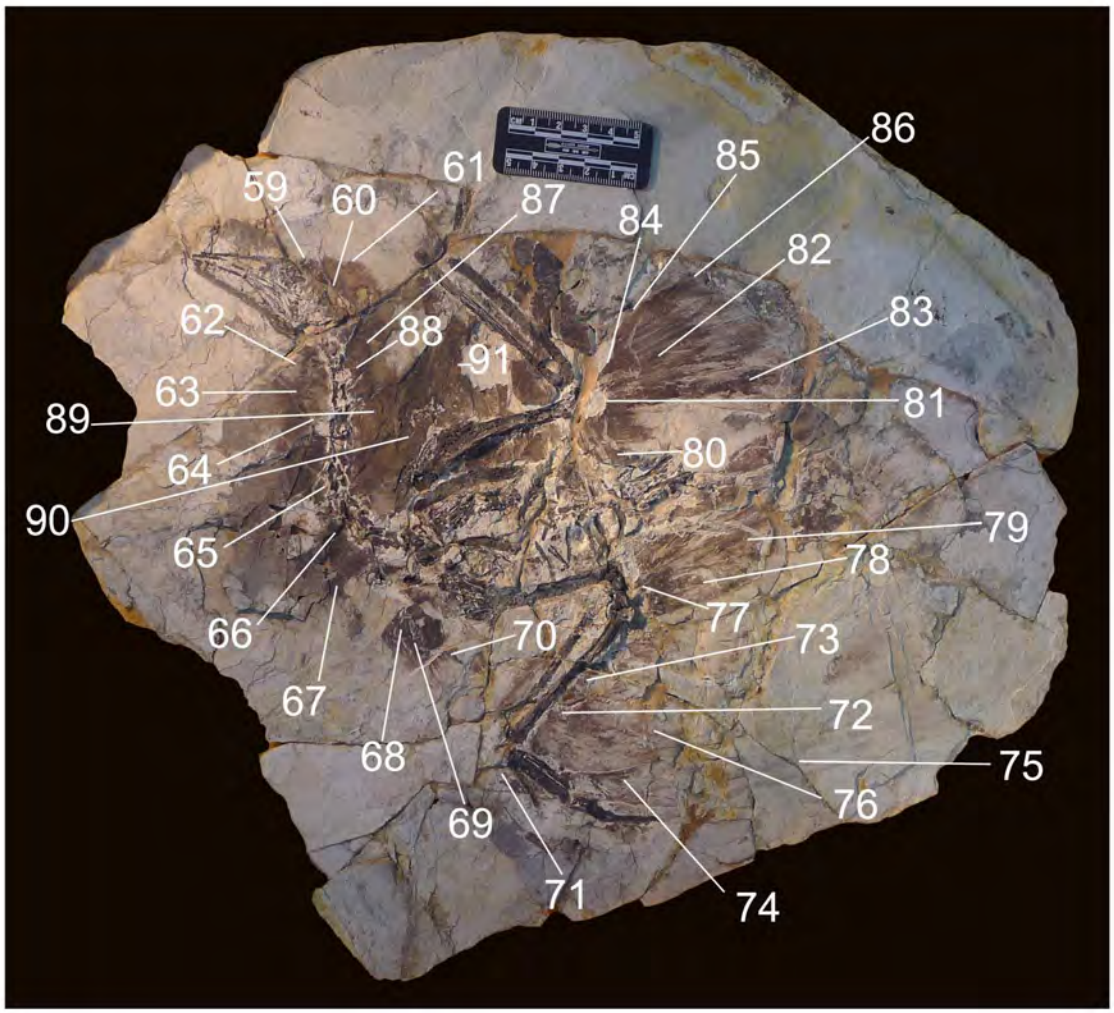

Extended Data Figure 8 | Sampling map of an undescribed ornithurine bird, CUGB G20100053. Numbers indicate integument sampling sites; melanosome data from all sites are presented in Fig. 4 and pooled for the per-taxon values given in Supplementary Table 2.

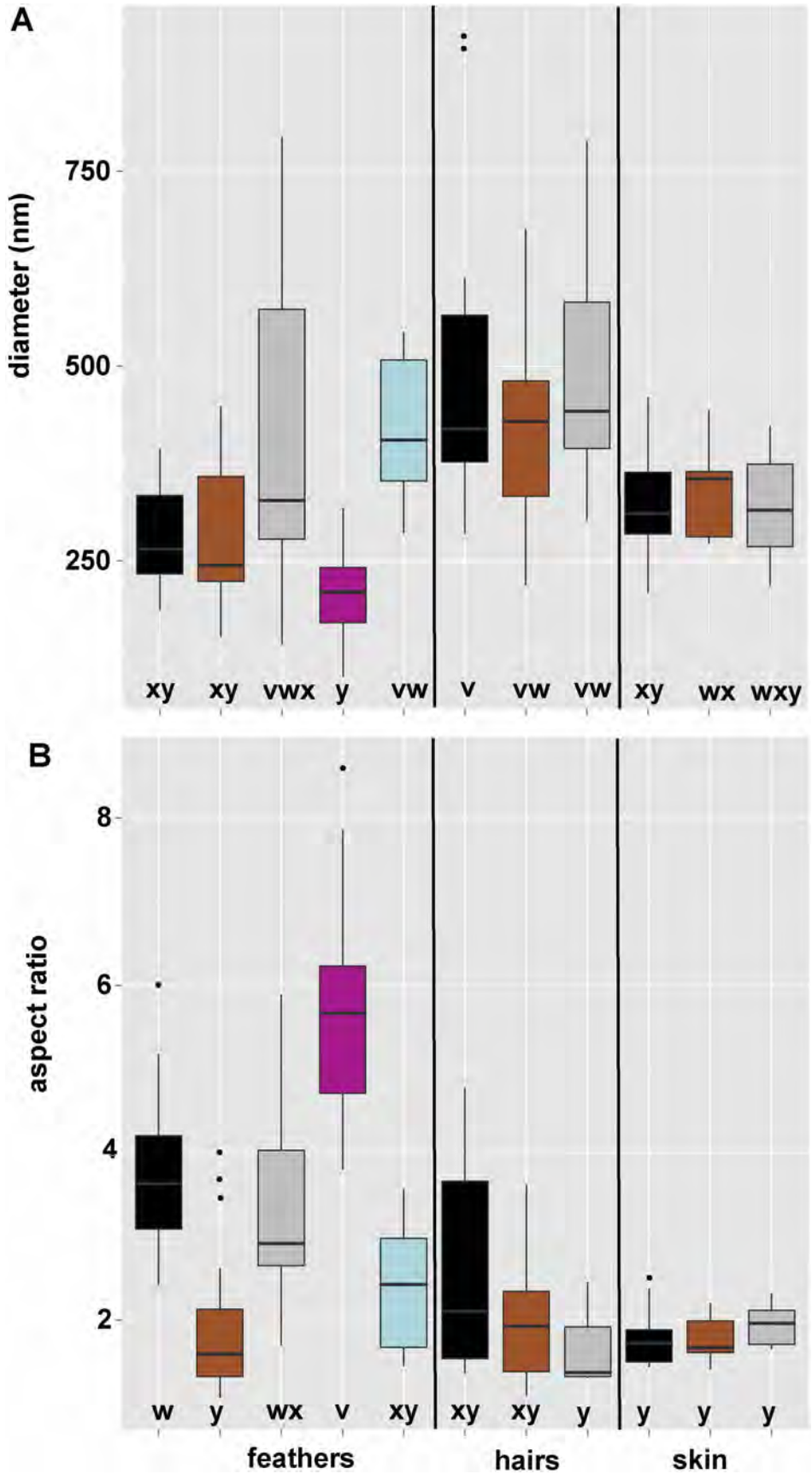

Extended Data Figure 9 | Melanosome diameters and aspect ratios observed in extant feathers, lepidosaur, testudine and archosaur skin, and mammalian hair. Melanosome diameters are shown in **a**, and aspect ratios are shown in **b**. Boxplot colours correspond with integument colour: black, brown, grey. For feathers, 'penguin-like' is shown in blue and iridescent is shown in purple. Lines are median values, boxes are quartiles, lines are range. Boxplots sharing the same letter (v, w, x, y, z) are not significantly different from one another.

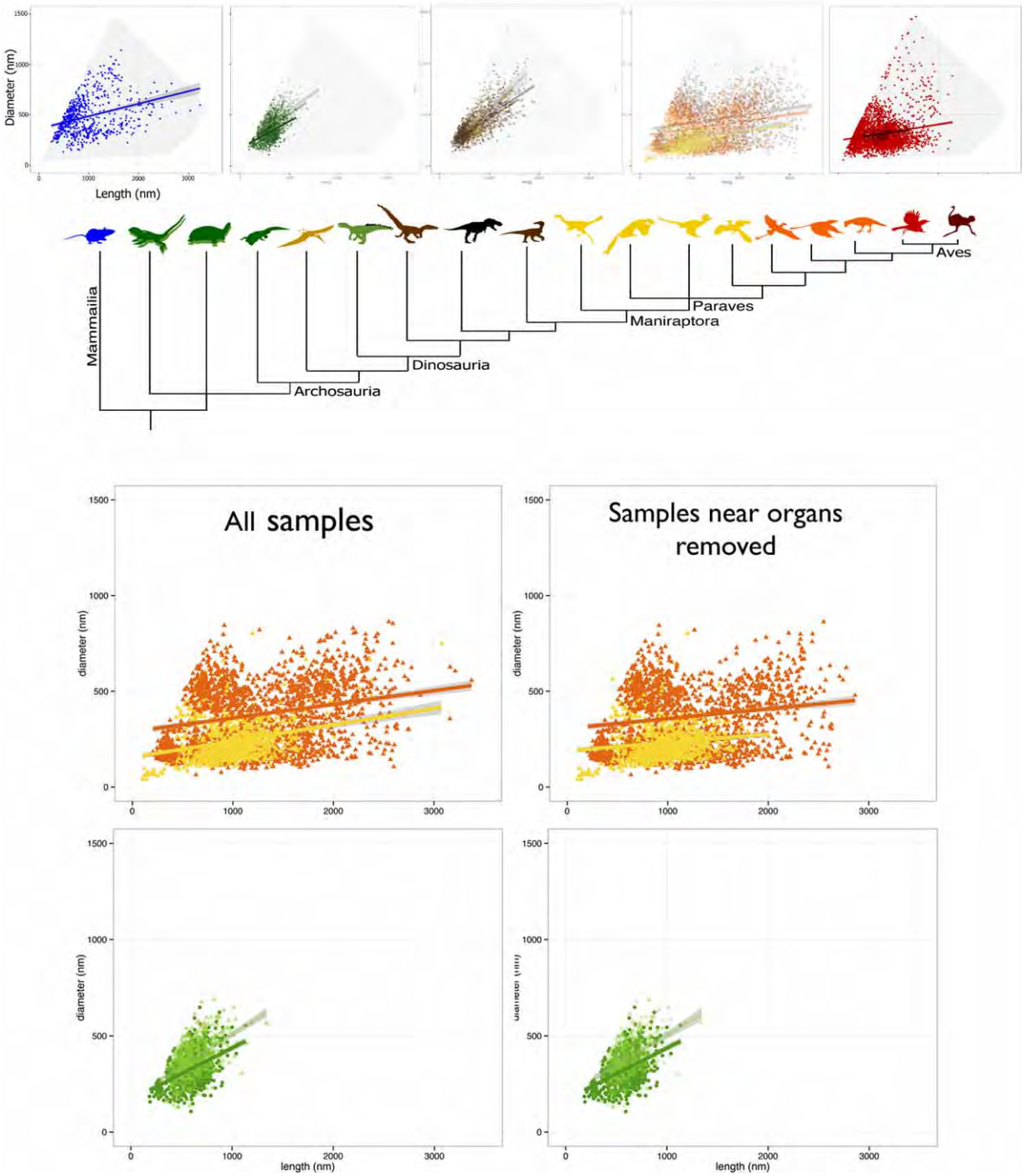

Extended Data Figure 10 | Exploration of the potential effects of taphonomy and sampling on the observed differences in melanosomes in skin, hair, filaments and feathers. Top, melanosome diversity is adjusted to model taphonomic shrinkage of melanosomes suggested from experimental studies. Values for all fossil samples were adjusted (enlarged by 20%) based on the findings of ref. 18 (Supplementary Methods). Original data points are shown in colours and adjusted data are shown in grey. Grey regions indicate the extent of the total melanosome morphospace from the primary analyses. The pattern reported (i.e., increased diversity and higher-aspect-ratio forms only in Maniraptora and Mammalia) is not affected (Fig. 4, main text; *n* for each integumentary type is identical to the primary analysis). Bottom, to consider the effect of sampling on the observed pattern samples from near the thoracic region were removed from the database. Although there was no evidence to suggest that these samples were from internal organs, or that such organs were preserved, because melanosomes are present in some internal organs in extant taxa, the sensitivity of the results to removal these samples was explored. There was no effect on the pattern reported from the primary analysis (compare Fig. 4). Samples 1 and 2 from *Yabeinosaurus* sp. (PKUP V1059), sample 1 from *Psittacosaurus lujiatunensis* (PKUP V1050), samples 121, 122 and 123 from *Caudipteryx zoui* (PMOL AD00020), samples 11, 13 and 14 from an undescribed enantiornithine (CUGB P1201), samples 30 and 33 from an undescribed enantiornithine (CUGB G20120001), and samples 64–69, 89 and 90 from an undescribed ornithurine bird (CUGB G20100053) were removed from the database. Samples are colour coded as in Fig. 4, main text and adjusted *n* for subsampling analysis follows: extant mammal hair (blue, $n = 719$), skin from extant (dark green, $n = 742$) and extinct (light green, $n = 605$) lepidosaurian, testudine and archosaurian species, feathers in basal Paraves (yellow, $n = 1{,}212$), *Confuciusornis* and crown-ward extinct avialan taxa (orange, $n = 1{,}376$), extant Aves (bright red, $n = 3{,}294$) and flightless palaeognath birds (dark red, $n = 107$). Colours of silhouettes correspond with colours in scatterplots. Black indicated unsampled taxa or integumentary type (e.g., bristle structures on the tail of *Psittacosaurus*).